Tomographic modeling of GNSS ionospheric corrections: Assessment and real-time applications

M. Hernández-Pajares, J. M. Juan, J. Sanz, *Depts. of Applied Mathematics IV and Applied Physics, group of Astronomy and Geomatics, Universitat Politècnica de Catalunya (gAGE/UPC), Barcelona, Spain*

O.L.Colombo, *GEST/NASA GSFC, Maryland, USA*

BIOGRAPHIES

Dr. Manuel Hernández-Pajares is associate professor in the Department of Applied Mathematics IV at the Universitat Politècnica de Catalunya since 1993. He started working on GPS in 1989, for cartographic and surveying applications, and now he is currently focused on the area of GNSS ionospheric and atmospheric determination, and precise radionavigation.

Dr. J. Miguel Juan Zornoza is an associate professor in the Department of Applied Physics at the Universitat Politècnica de Catalunya. His current research interest is in the area of GPS ionospheric tomography, GPS data processing algorithms, and radionavigation.

Dr. Jaume Sanz Subirana is an associate professor in the Department of Applied Mathematics IV at the Universitat Politècnica de Catalunya. His current research interest is in the area of GPS ionospheric tomography, GPS data processing algorithms, and radionavigation.

Dr. Oscar L. Colombo works on applications of space geodesy, including gravity field mapping, spacecraft orbit determination, and precise positioning by space techniques, mostly for the Space Geodesy Branch (Code 926) of NASA Goddard Space Flight Center. In recent years, he has developed and tested techniques for very long baseline kinematic GPS, in collaboration with groups in Australia, Denmark, Holland, and the USA.

ABSTRACT

It has been demonstrated in previous work that the tomographic approach reduces significantly the mismodelling in the electron content determination with Global Navigation Satellite Systems like GPS. We present in this paper the results of an comprehensive study about the performance of a tomographic model of the ionosphere, computed from the L1 and L2 carrier phase data, in order to estimate undifferenced and double differenced ionospheric corrections.

Firstly, previous work has shown that the comparison with the TOPEX-Poseidon altimeter TEC for more than 2.5 years of data, including Solar Maximum (June 1998 to 2001), presents errors of few TECU at mid and high latitudes for the post-processed TEC computed from GPS data, and 5-10 TECU in equatorial regions. The real-time TEC computed close to equatorial regions, using the ambiguities fixed in the ionospheric model, is better than those post-processed results. During four consecutive weeks in March-April 2001, under Solar Maximum conditions, including some days of high geomagnetic activity, the STEC errors are less than 5 TECU and about 1 TECU for double differenced STEC, with reference stations separated 1000 to 3000 km, and close to the southern Appleton anomaly. These results strongly suggest that these models can improve significantly both navigation and time transfer with single frequency receivers, even in equatorial regions.

Secondly, the real-time doubledifferenced ionospheric corrections have been studied for six different scenarios at medium and high latitudes during 17 different days in 1999, 2000 and 2001, and including different ionospheric conditions, such as geomagnetic activity and Traveling Ionospheric Disturbances (TIDs). The results for the WADGPS-like scenarios indicate that the tomographic model is accurate enough (better than 0.25 TECU for the rover receivers) to solve on-the-fly the carrier phase ambiguities, at distances of hundreds of kilometers of the nearest reference receiver, allowing for example very precise navigation (errors below 10 cm), and real-time tropospheric determination within WADGPS networks.

INTRODUCTION

As demonstrated in recent years, it is possible to provide ionospheric corrections from GNSS systems such as the Global Ionospheric Maps computed from GPS data (see for example Wilson et al. 1995). In the case of real-time applications such as wide-area navigation augmentation systems (WAAS, EGNOS..., see for example Hansen et al. 1999) the ionospheric corrections have to be calculated from stations typically separated several hundreds km or more, with only the data gathered until the present epoch. This limitation usually produces worst results than computing the ionospheric corrections in post-process. One way to overcome this natural limitation is to run also, simultaneously, a geodetic program solving the carrier phase biases. Combining both complementary types of information, the ionospheric corrections and also the geodetic outputs can improve significantly. Some examples of that can be found in Hernández-Pajares et al. 2000b for ionospheric corrections, in Colombo et al. 1999 for navigation and in Hernández-Pajares et al. 2001 for real-time tropospheric determination.

The purpose of this paper is to show the synergy between precise ionospheric modeling, with the benefits of a tomographic approach, and precise position determination, in real-time, and using reference GNSS stations separated by hundreds of kilometers, or more. This includes Wide Area Differential GNSS (WADGNSS)-like networks, for example WAAS, EGNOS or MSAS, in which this combination of techniques makes feasible, for example, On-The-Fly ambiguity resolution for roving receivers (top plot of figure 1, and details in Colombo et al. 2000) with position accuracies below 10 cm, or the real-time tropospheric estimation (bottom plot of figure 1, and details in Hernández-Pajares et al. 2001). And, at larger distances, this can help to improve the accuracy in real-time global ionospheric maps, that may be feasible very soon with the shift of the International GPS Service (IGS) towards real-time capabilities (Zumberge et al. 1999). These maps can help to improve the accuracy for single-frequency users.

The paper is organized as follows: In the first part, after the description of the technique, an overview will be given of several successful and already reported experiments of this strategy, in different WADGNSS-like scenarios. In the second part of the paper, two new studies, that improve the availability of the precise ionospheric corrections, will be presented in detail. The first one shows the effectivness of the technique in resolving ambiguities on the fly in the presence of local ionospheric irregularities, such as Traveling Ionospheric Disturbances (TID's). This first experiment was performed in 1999, with the rover at distances of more than one hundred kilometers from the nearest reference receivers, and at high northern latitudes. The second experiment tested the improvement of real-time ionospheric determinations, using data from GPS permanent stations from one thousand to three thousand kilometers apart. This four-week experiment took place in 2001, under hard ionospheric conditions: in the equatorial region near Solar Maximum.

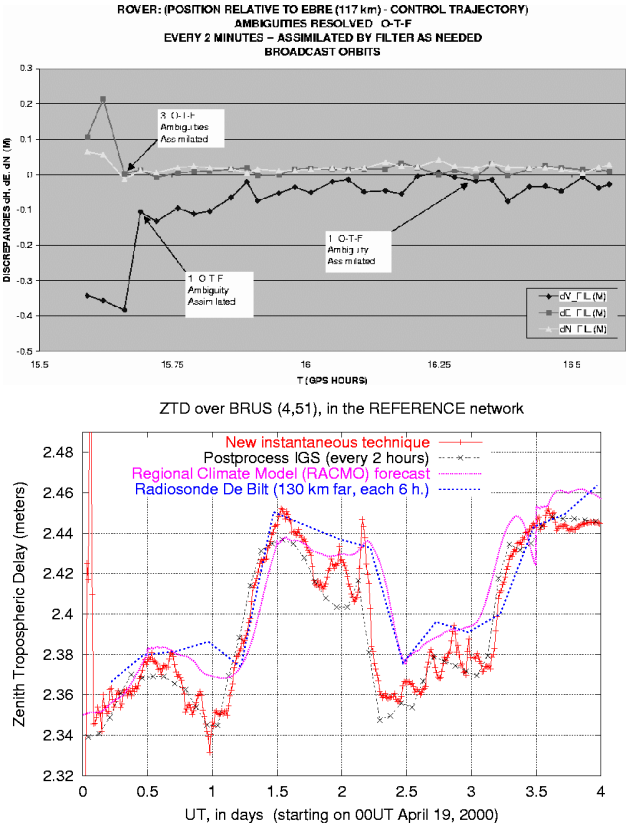

Figure 1: Two recent applications of the capability to solve in real-time the double-differenced carrier-phase ambiguities by means of the real-time ionospheric corrections computed using the WARTK technique described in the paper: In the upper plot, the errors in the navigation of a rover (a car in this case) are less than 10 cm in the three components -North, East and Up- (experiment "Bellkin'99", in table 1). The lower plot shows the difference between the real-time vertical tropospheric delay and (a) the IGS combined post-processed, (b) radiosonde measurements and (c) numerical weather model predictions. The errors are typically less than 1cm (experiment "SolarMax-1", No.4 in table 1).

DESCRIPTION OF THE TECHNIQUE

The free electron ionospheric distribution is approximated by a grid of voxels in which the electron density is assumed constant at a given time in an Earth Centered Inertial (ECI) system (see a typical layout in figure 2). The ionospheric determination is performed solving in real-time, by means of a Kalman Filter (Bierman, 1977), the mean electron density N_e of each illuminated cell *i,j,k* (in solar longitude, latitude and

height respectively), treated as a random walk process, and with typical process noise of 10^9 -10^{10} electrons/m^3 /$\sqrt{hour}$. The carrier phase data are the only ones used. Then the pseudorange code noise and multipath are avoided. The carrier phase biases B_I (constant in each given continuous arch of carrier phase data for each satellite-receiver pair) are estimated simultaneously as random variables (that become white noise random processes when a cycle-slip happens). In the filter the biases decorrelate in real-time from the electron density values, as far as the satellite geometry changes and the variance of both kind of unknowns became smaller (see equation 1 that represent the model for a given ionospheric datum, between one GNSS satellite and one receiver, being L_1 and L_2 the carrier phases in length units, L_I=L_1–L_2 and N_e the electron density).

$$L_I = STEC + B_I = \int_{REC}^{SAT} N_e dl + B_I = \\ = \sum_i \sum_j \sum_k (N_e)_{i,j,k} \Delta s_{i,j,k} + B_I \qquad (1)$$

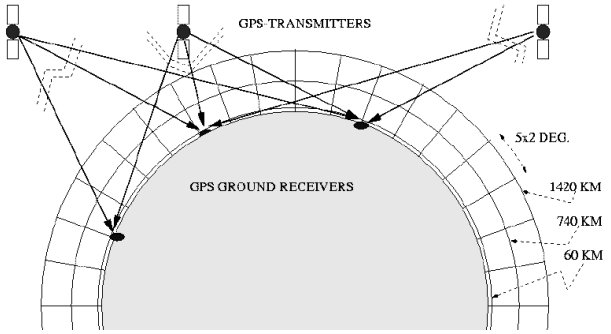

Figure 2: Meridian slice of the voxels in which the ionospheric electron density distribution is decomposed, in the GNSS data driven real-time model, equation 1.

This approach is suitable in particular to detect local features of the electron density distribution, and the use of two layers with ground GNSS data –instead of one as is typically done by many authors– reduces significantly the mismodelling of the electron content determination (Hernández-Pajares et al. 1999a-b)

In the case of WADGNSS networks, from these real-time slant total electron content (STEC) corrections obtained by equation 1, it is possible: Firstly (see flow chart in figure 3), to form the station-satellite double differences, $\nabla\Delta STEC$, and to obtain a second ambiguity (the widelane) in the reference stations, and, secondly (see flow chart in figure 4), to interpolate to the rover the unambiguous LI, i.e. a very precise $\nabla\Delta STEC$ to the level of few tenths of TECU[1]. If the interpolated value is better than 2.7 cm ≅ 0.25 TECU, then the rover will be able to solve both ambiguities in real-time. This and another details of the technique, hereinafter Wide Area Real Time Kinematics (WARTK), can be found for instance in Hernández-Pajares et al. 2000a, 2000b.

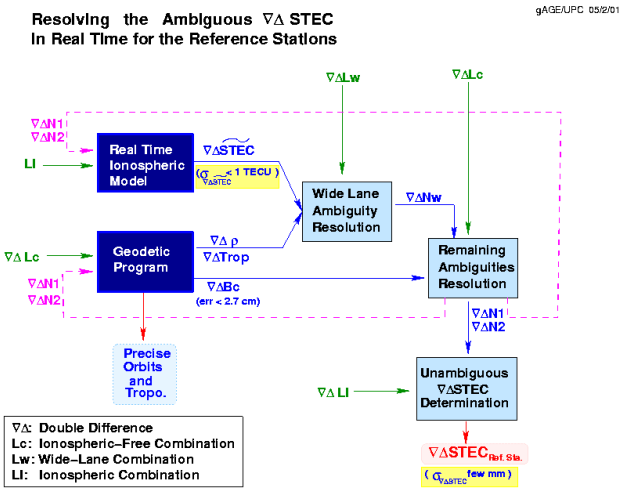

Figure 3: Flow diagram of the main processing steps for the reference stations.

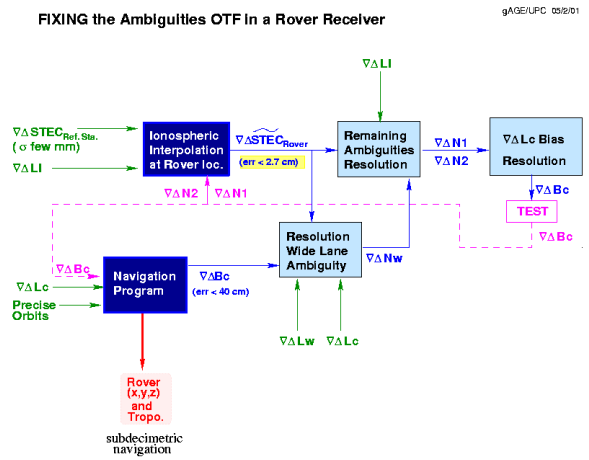

Figure 4: Flow diagram of the main processing steps for the rover (user).

The results obtained so far with the WARTK technique, in different experiments, are summarized in table 1.

[1] 1 TECU = 10^{16} electrons/m^2 ≅ 10 cm in L_1 - L_2 ≅ 15 cm in L_1 ≅ 20 cm in Lw (widelane combination).

No.	Exp.	Ionos. Activity	Distances (km) Rover/Ref.	Ref. Succes	Rover Success	Kind Rover	Dates	Region	Reported in
1	BelKin99	Quiet	116/ 286	97%	80-100%	Car	March 23, 1999	Spain NE	Colombo et al. 1999
2	NWPacific (1)	Active Kp=6	400/ 900	90-100%	80%	IGS Site	May 3, 1998	Canada -USA NW	Hernández-P. et al. 2000a Colombo et al. 2000
3	NWPacific (2)	Irreg. Apr30	162/ 900	95-100%	80-90%	IGS Site	Apr28 to May 1, 1998	Canada -USA NW	Hernández-P. et al. 2000b
4	SolarMax (1)	Solar Max.	130/ 500	85-95%	80%	IGS Site	Apr 19 -22, 2000	Central Europe	Hernández-P. et al. 2001
5	SolarMax (2)	Very Active	130/ 500	50-95%	80%	IGS Site	Jul 12 -15, 2000	Central Europe	Hernández-P. et al. 2000b
6	Baltic99 (1)	TID's	144/ 285	97%	83%	Fixed Site	Aug 25, 1999	North Europe	This paper
7	Equator01	S.Max. Equat. Kp:0-9	1000-3000	90%	-	IGS Site	Mar6 to Apr 2, 2001	Asia-Oceania	This paper

Table 1: Summary of the experiments performed so far to quantify the performance of the real-time tomographic model of the ionosphere and the associated WARTK technique. More details can be found in the references indicated in the last column.

For the kinematic use of the algorithm one of the strongest limits is the existence of local ionospheric irregularities, such as Traveling Ionospheric Disturbances (TID), that can produce poor results using a linear interpolation of the ionospheric corrections between the reference stations. We will improve the performance incorporating the rover dual frequency data (Hernández-Pajares et al. 2000b). On the other hand, in the case of the reference stations calculation, the long distances and strong electron content gradients can limit the performance of the technique. For this reason, we extend in this paper the algorithm to include the case of permanent/reference stations separated thousands km, using widelane-smoothed code to improve the ionospheric model and hence to help achieve real-time ambiguity determination.

NEW EXPERIMENT (BALTIC'99): ROVER ALGORITHM WITH TRAVELING IONOSPHERIC DISTURBANCES

The purpose of this experiment is to show the performance of the WARTK algorithm, especially in the interpolation of the precise $\nabla\Delta STEC$ from the reference stations to the rover in the presence of local ionospheric irregularities.

DATA DESCRIPTION

The data were collected at seven fixed dual-frequency GPS receivers in the Baltic Sea region, in August 25th 1999, from 06 to 11 hours UT. The seven included IGS stations VIS0, MAR6, VIRO and LAMA (recording each 30 sec.), and the fixed stations TUOR, HIIU and MHN2 (recording each 1 sec.), as part of a remote-sensing flight with onboard GPS receivers. In what follows, the fixed receiver MHN2 is treated as rover and, as it can be seen in the corresponding map, figure 5, the typical distances between the reference receivers are 200-400 km, and between the rover and the closest receivers are 150-200 km.

DISCUSSION AND RESULTS

From previous studies (experiments 2 and 3 in table 1), the resolution of the reference stations ambiguities normally should not be a problem in this scenario, at high latitude and low geomagnetic activity (a success close to 100% of the attempts made at every epoch to resolve the ambiguities is attained).

But the situation is complicated by the occurrence of Traveling Ionospheric Disturbances (TID's) affecting the signals of most of the GPS satellites observed during the flight. An example of the observed ambiguous STEC (L_I) for satellite PRN25 is shown in the first plot of figure 6. Oscillations reaching 20 cm can be observed with different intensity and relative phase depending on the observer's position, and hence depending on the station. An example of the direct impact of these TID's in the $\nabla\Delta STEC$ interpolation to the rover can be also seen in figure 6, second plot. The linear interpolation between the three surrounding reference stations MAR6, HIIU and TUOR -the reference for the double differences- (see map in figure 5) produces errors greater than 2.7 cm compared to the true $\nabla\Delta STEC$ as observed at the rover. An error of that size causes one or more cycles of error in both the

L_1 and L_2 ambiguities of the rover. When the dual-frequency data of the rover receiver, MHN2, are also used in the WARTK technique, as it is indicated in figure 4, the results are significantly better, with errors typically below 2.7 cm.

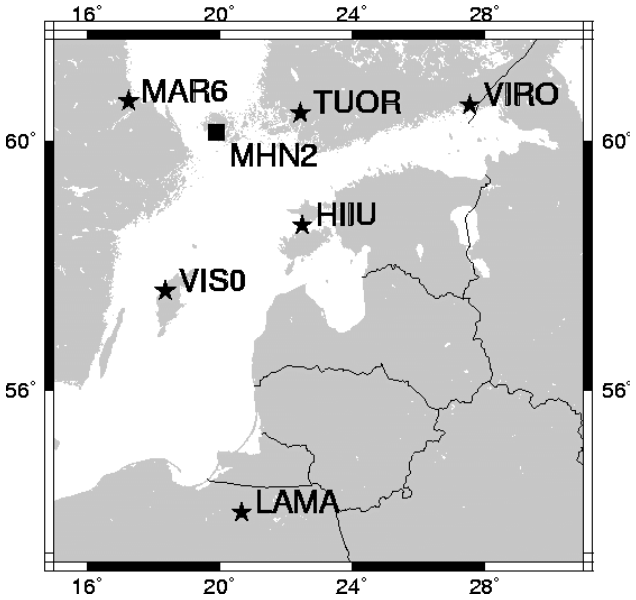

Figure 5: Map with the fixed reference stations (stars) and the fixed station MHN2 treated as rover (square), used in the experiment in which the ionosphere presents TID's (August 24, 1999).

An overall picture of the performance for all the satellites can be seen in figure 7, in which the errors in $\nabla\Delta STEC$, and corresponding success rate in full (L_1 and L_2) ambiguity resolution for the rover are plotted, with an overall success of 83% of attempts made at all epochs. However, linear interpolation gives just a 49% of success in this scenario.

NEW EXPERIMENT (EQUATOR'01): LOW-LATITUDE SCENARIO WITH LONG DISTANCES AND AT SOLAR-MAXIMUM

The strategy discussed so far has been used previously only at mid and high latitudes with typical distances of 100-500 km between receivers, and under various ionospheric conditions, giving in all cases good results (see summary in table 1).

The goal of this new experiment is to assess the performance of the real-time ionospheric model at greater distances, 1000-3000 km, over a wider range of latitudes and over a longer period of time, under some very active ionospheric conditions.

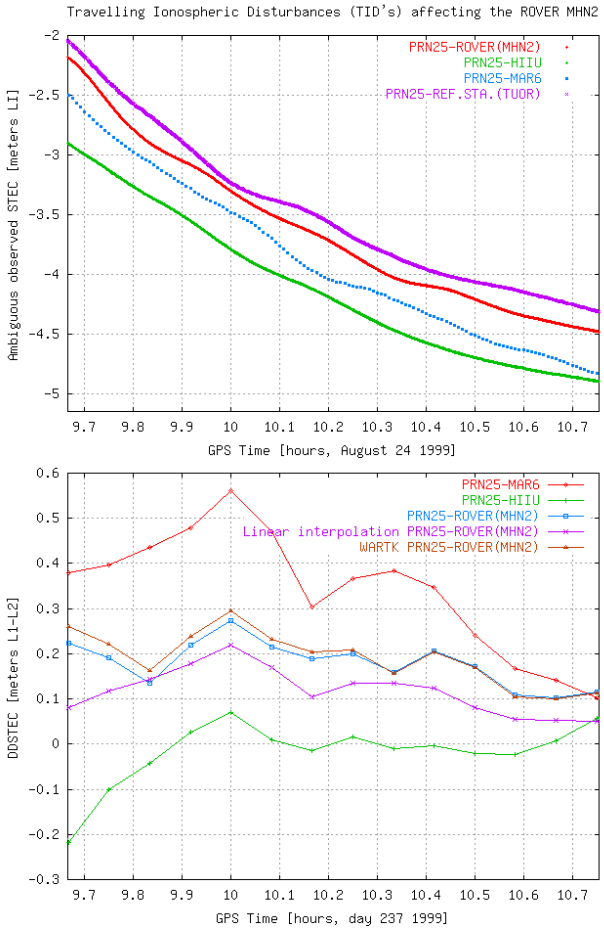

Figure 6: Example of TID's observed in satellite PRN25, from the rover station (MHN2), and the reference stations MAR6, HIIU and TUOR (the reference for the double differences). In the top figure the ambiguous STEC's are plotted, in which the propagation of the TID's can be observed. And in the bottom figure, we can see the TID's impact on the double differences, as they affect the performance of the linear interpolation done to provide $\nabla\Delta STEC$ corrections to the user. The TID's affected more than 50% of the GPS satellites measured in this experiment.

DATA DESCRIPTION

The data corresponds to a set of 12 permanent IGS receivers in Asia and Australia, shown on the map of figure 8. The TOPEX-Poseidon TEC observations are also used as "truth" (see typical footprints in the same figure). It can be seen in the figure that, at these latitudes, this distribution covers both ionospheric equatorial anomalies, and that the distances between sites are in the range of 1000-3000 km.

The data period spans four whole consecutive weeks, from March 6th to April 2nd of 2001, i.e. close to the Solar Maximun, and includes the Spring seasonal maximum of the noon TEC, and several disturbed periods (see Kp index in figure 9).

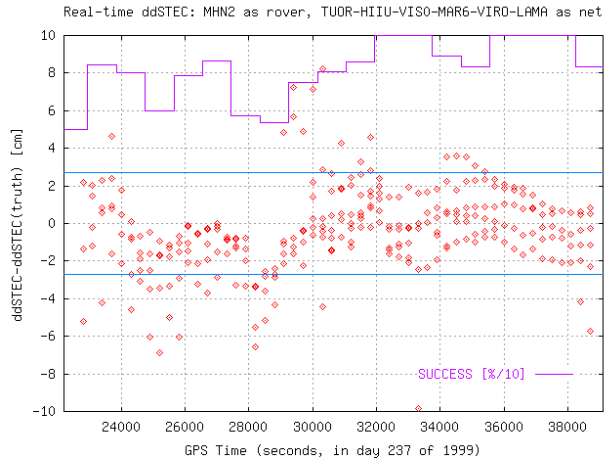

Figure 7: Error of the double differenced STEC for the fixed site MHN2, treated as rover, in function on the time. Also, the success percentage is plotted each 15 minutes. The overall performance is the 83% of success (regarding on all the available satellites) in providing an ionospheric correction precise enough to determine the two rover carrier phase ambiguities (i.e. better than 2.7 cm). When an alternative linear interpolation method is used, the success decreases to 49%. The corresponding performance for one-cycle of maximum common error in both ambiguities of L1 and L2 is 99% for WARTK and 92% for linear interpolation.

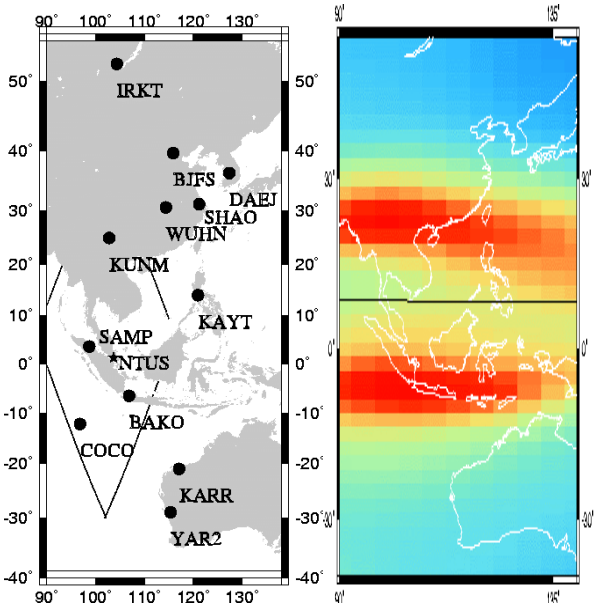

Figure 8: Left plot: IGS stations used in the study of precise ionospheric determination performed during 4 consecutive weeks, between March and April 2001 (the TOPEX tracks compared for the day 67 are also plotted). Right plot: the TEC during the local afternoon (07UT, day 67, March 8th, 2001) and the geomagnetic equator are also represented. The units are tenths of TECU (1 TECU = 10**16 electrons/m**2 ≅ 15 cm in L1). The Appleton north and south tropical anomalies are clearly present, where the TEC reaches values of more than 120 TECU or more, compared to 90 TECU between them, and 60 TECU or less in the north and south edges of the map (source: UPC GIM).

STRATEGY

In the works mentioned earlier, it has been shown that ambiguity resolution requires the accuracy of the $\nabla\Delta STEC$ correction for the rover to be better than 2 TECU (i.e, a one-sigma precision of 1 TECU). Furthermore, with distances of less than 1000 km between reference stations a success rate higher than 90% can be obtained. This is better by 10% approximately than the rate for the use of the smoothed pseudorange to calculate the wide-lane ambiguity. However, at still greater distances (more than 1000 km) and with high ionospheric variations one can expect a lower percentage. In this case the smoothed code can be useful to help fix the widelane ambiguities, and to slightly constrain the estimation of the real-time ionospheric model.

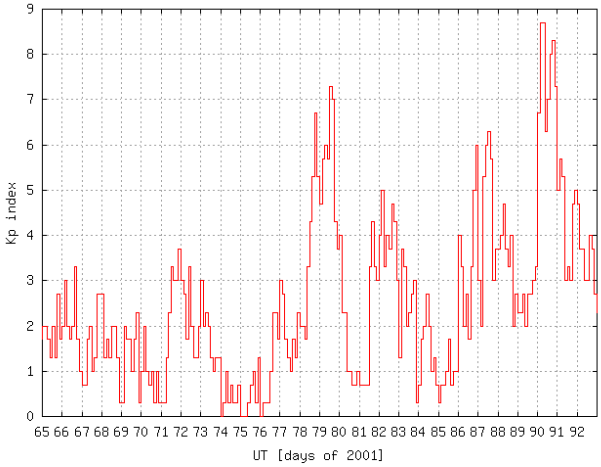

Figure 9: Kp index reflecting the geomagnetic activity for the period of 4 consecutive weeks studied in the second experiment presented in this paper. During the first two weeks aproximately (DOY's 65-77) the geomagnetic activity is low to moderate (Kp <4). However, the last two weeks (DOY's 78-92) the geomagnetic activity attain high and extreme values in certain periods, with 6 < Kp < 9.

The main problem using smoothed code is the presence of multipath, but for permanent receivers it is possible to choose a good antenna location to mitigate this problem. And it is also possible to use the receiver data to estimate the actual antenna multipath pattern in order to correct and strongly diminish the code multipath effect. Only three of the receivers multipath (BJFS, KAYT and SHAO) has been mitigated subtracting a model, obtained from the carrier phase.

RESULTS

The precision of the real-time ionospheric corrections based on carrier phase data from reference stations at very long distances from each other (1000-3000 km) can be assesed in three different ways, for the vertical TEC, the STEC and the $\nabla\Delta STEC$:

First they are compared to the available precise TEC estimates obtained directly from the dual-frequency altimeter on the TOPEX-Poseidon satellite over seas close to the GPS permanent receivers (figure 8).

Two examples of direct comparison of vertical TEC are shown in figure 10, for geomagnetically quiet and very active conditions (days 67 and 90, 2001, with Kp in the ranges 0-3 and 6.5-8.5 respectively, see figure 9). In general the real-time TEC follows the main trends of TOPEX TEC but with higher values, this discrepancy being compatible with the presence of a plasmaspheric electron content between the altimeter and the GPS satellites. This performance can be still better than the post-processed results, such as distributed UPC Global Ionospheric Maps (GIM) (see Hernández-Pajares et al. 1999a for more details), or any of the available GIM's of other centers (in "IONEX" ionex format, on-line at *ftp://cddisa.gsfc.nasa.gov/pub/gps/products/ionex/YEAR/DOY*). The reason for that is the improvement due to fixing the ambiguities in real-time (figure 3).

A summary of this comparison for the first two weeks of this study, with lower geomagnetic activity, and also for the last two weeks with higher activity, confirms these results. Figure 11 shows the bias and standard deviation of the difference TEC[GPS]-TEC[TOPEX] plotted as a function of latitude, for the two daily TOPEX passes near local noon (top plot) and local midnight (bottom plot), with TOPEX observations relatively close to GPS stations.

A second comparison can be made between the observed ambiguous STEC value with its real-time prediction, for a receiver that has not been used in the computations. This is the case for the IGS station NTUS, separated by approximately 600 km from the nearest station, SAMP (see map in figure 8). It can be seen in figure 12 that the variation of STEC can be well predicted, to better than 5 TECU.

Finally, in a third study of the performance of this approach the RMS of the error in $\nabla\Delta STEC$ prediction has been calculated using a post-processed solution as "truth", and then compared to the corresponding success rate in widelane ambiguity resolution (see flowchart in figure 3). It can be seen in figure 13 the results for a baseline of 2354 km (COCO-KARR), and under the influence of the southern Appleton anomaly: the RMS is typically about 1 TECU, and the success rate is greater than the 90% during the four consecutive weeks of the period studied, with a mean rate of 97%. That period includes days of high geomagnetic activity, as shown in figure 9. These results are quite representative, as it can be seen in in table 2, for a set of baselines, for both northern and southern tropical ionosphere.

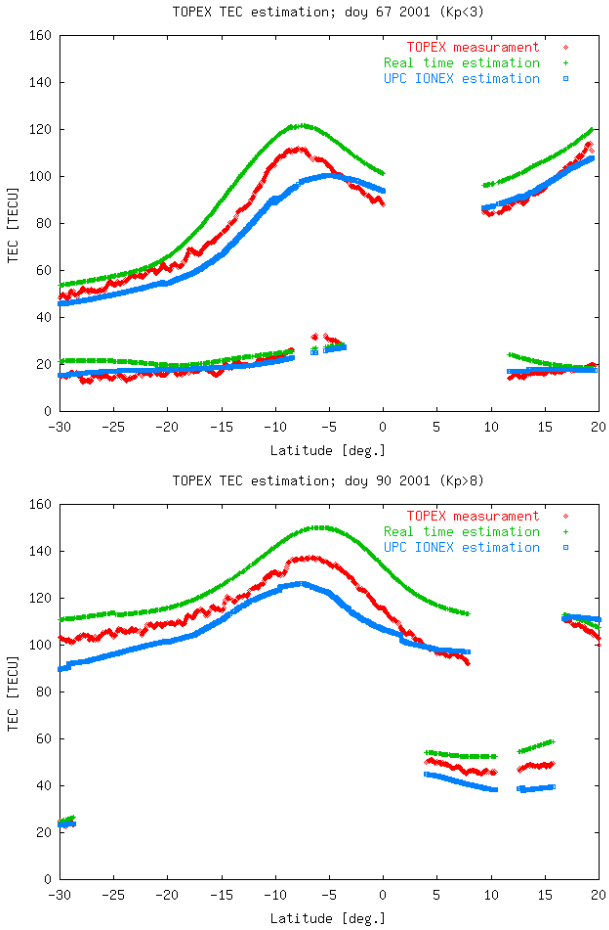

Figure 10: Comparison of real-time ionospheric vertical TEC determination, and post-processed solution, both with GPS data, and TOPEX TEC for a geomagnetically quiet day (March 3rd, 2001, top plot), and a day geomagnetically very disturbed, with Kp ≅ 8 (March 31st, 2001, lower plot).

SUMMARY AND CONCLUSIONS

The Wide Area Real Time Kinematic (WARTK) algorithm performs well when used to compute precise real-time ionospheric corrections in WADGPS-like networks. In several experiments previously reported in other publications, the WARTK provided $\nabla\Delta STEC$ better than 2.7 cm (1/4 TECU) for the reference and rover receivers, in middle and high latitudes, and under different ionospheric conditions.

The more challenging part of the technique, the interpolation of the precise $\nabla\Delta STEC$ from the reference stations to the rover, has been successfully tested in this paper in a difficult situation, with strong local irregularities in the ionosphere (TID's), while nevertheless doubling the performance compared to a standard linear interpolation technique (success of 83% vs 49%, respectively).

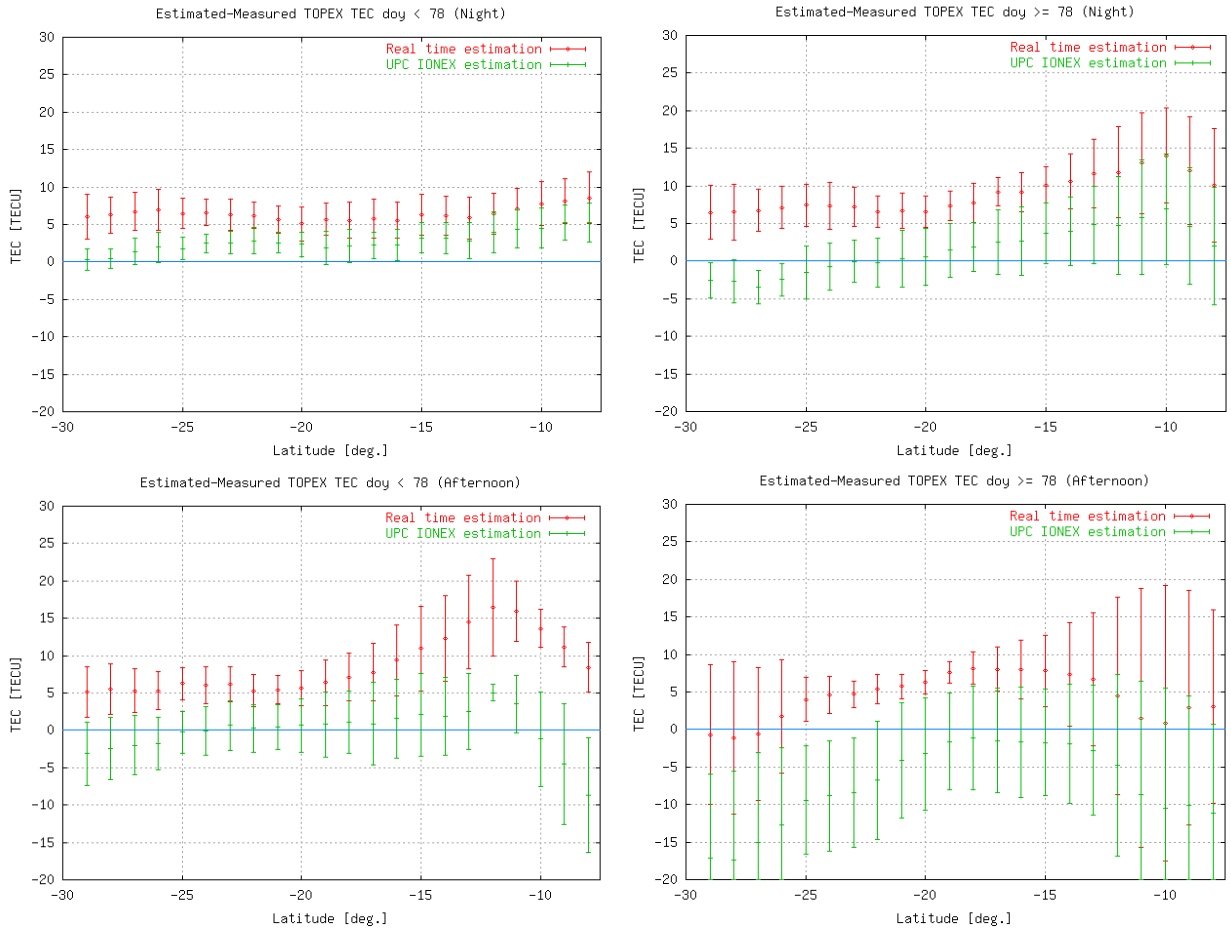

Figure 11: Bias and standard deviation (represented as bar errors) of the differences between GPS TEC and TOPEX TEC for the first part of the studied period with low geomagnetic activity (before DOY 78, March 19th 2001, first column) and with higher geomagnetic activity (starting on DOY 78, second column), during the local night (22-04LT, first row) and during the local afternoon (12-18LT, second row).

The improvement in real-time STEC determination for the reference GPS stations has been also studied in this paper, in one of the worst possible scenarios: very long baselines (1000-3000 km), at low latitudes, and near-Solar Maximum conditions, during four consecutive weeks, including periods of high geomagnetic activity (March-April 2001). The vertical TEC prediction for the TOPEX-Poseidon satellite made with this method was larger than the TEC actually observed with the TOPEX-Poseidon dual frequency altimeter. This discrepancy is compatible with the existence of a significant plasmaspheric electron content between the TOPEX and the GPS satellites. This result is more compatible with TOPEX than the post-processed one at global scale (GIM's), without fixing ambiguities. The standard deviation of the discrepancies with the TOPEX vertical TEC is at the level of 1-3 TECU. This result is compatible with the agreement observed between measured and predicted STEC for GPS receivers not involved in the computations. Finally, in this study the RMS of the difference between the $\nabla\Delta STEC$ and the post-processed "truth" is about 1 TECU, and the success rate in ambiguity resolution is greater than 90%. Similar results have been achieved for pairs of stations separated by more than 2000 km, and experiencing the strong gradients of the southern equatorial anomaly. Data from further experiments involving moving receivers on airplanes, boats and cars, are being analyzed at the present time.

ACKNOWLEDGMENTS

The authors thank to Dr. Rene Forsberg and Dr. Arne Olesen (KMS, Denmark) for making available their GPS data for Baltic region. The authors are grateful to the International GPS Service and cooperating organizations, for making publicly available the IGS data sets. The maps have been generated with the software package GMT (Wessel and Smith, 1995). Some geodetic calculations were made using the GIPSY software (Webb and Zumberge, 1997). This work has been partially supported by the Spanish projects PEN-005/2000-I, TIC-2000-0104-P4-03 and the Spanish-USA project Fulbright 2000-001.

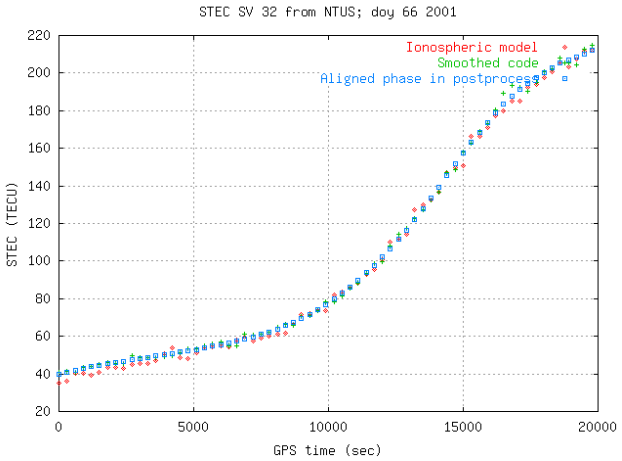

Figure 12: STEC predicted for NTUS, an IGS station not involved in the real-time determination over Asia and Australia, during the day March 7, 2001 (doy 66, March 7th, 2001).

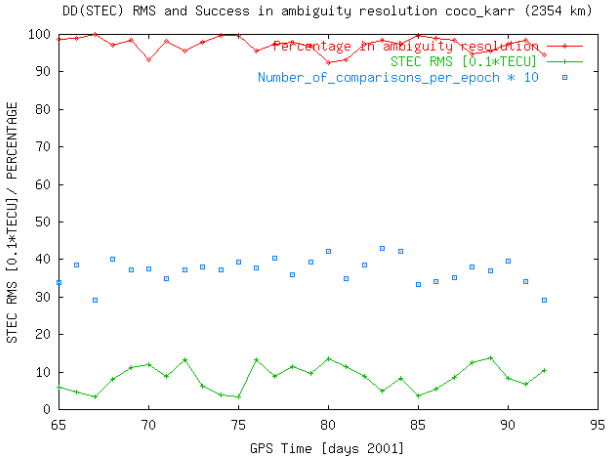

Figure 13: An example of the RMS of the $\nabla\Delta STEC$ real-time determination, and associated success for the double differenced widelane ambiguity, for the baseline from COCO (in the southern Appleton anomaly *footprint*) to KARR in Australia (2354 km away, bottom plot) since 6 March to April 2, 2001. The mean number of observations is also plotted for each day.

Sta.	Ref.	Dist. (km)	% Succ.	RMS [TECU]	# Obs.
IRKT	DAEJ	2507	93	1.2	8329
BJFS	DAEJ	1067	91	1.4	8131
KUNM	DAEJ	2640	95	1.0	3900
WUHN	DAEJ	1369	92	1.4	6358
SAMP	KARR	3341	95	1.1	6441
COCO	KARR	2354	97	0.9	9963
BAKO	KARR	1939	90	1.5	6121
YAR2	KARR	909	97	0.8	12630

Table 2: RMS of the $\nabla\Delta STEC$ real-time determination, and associated success for the double differenced widelane ambiguity, for a set of representative baselines. The distance, in km, and the number of observations are also indicated.

REFERENCES

Bierman, G.J., Factorization Methods for Discrete Sequential Estimation, Vol. 128 in Mathematics in Science and Engineering, Academic Press, New York, 1977.

Colombo, O.L., M. Hernández-Pajares, J.M. Juan, J. Sanz and J. Talaya, Resolving carrier-phase ambiguities on-the fly, at more than 100 km from nearest site, with the help of ionospheric tomography, ION GPS'99, Nashville, USA, September 1999.

Colombo O.L., Hernández-Pajares M., Juan J.M. and Sanz J., Ionospheric Tomography Helps Resolve GPS Ambiguities On-the-Fly At Distances of Hundreds of Kilometers During High Geomagnetic Activity, Position Location and Navigation Symposium (PLANS 2000 IEEE conference), San Diego (USA), March 2000.

Hansen A.J., T.F. Walter, P. Enge, Real-time Ionospheric Tomography Using Terrestrial GPS Sensors, Global Positioning System, Selected Papers on Satellite Based Augmentation Systems (SBASs), Vol. VI, The Institute of Navigation, Alexandria, USA, 1999.

Hernández-Pajares M., J.M. Juan and J. Sanz, New approaches in global ionospheric determination using ground GPS data, Journal of Atmospheric and Solar Terrestrial Physics. Vol 61, 1237-1247, 1999a.

Hernández-Pajares M., J.M. Juan, J. Sanz and O.L. Colombo, Precise ionospheric determination and its application to real-time GPS ambiguity resolution, Institute of Navigation ION GPS'99, Nashville, Tennessee, USA, September 1999b.

Hernández-Pajares, M., J.M. Juan, J. Sanz and O.L. Colombo, Application of ionospheric tomography to real-time GPS carrier-phase ambiguities resolution, at scales of 400-1000 km, and with high geomagnetic activity, Geophysical Research Letters, 27, 2009-2012, 2000a.

Hernández-Pajares, M., J.M. Juan, J. Sanz, O. Colombo, H. Van der Marel, Real-time integrated water vapor determination using OTF carrier-phase ambiguity resolution in WADGPS networks, ION GPS'2000, Salt Lake City, September 2000b.

Hernández-Pajares, M., J.M. Juan, J. Sanz, O.L. Colombo, and H. van der Marel, A new strategy for real-time Integrated Water Vapour determination in WADGPS networks, Geophysical Research Letters, 28, 3267-3270, 2001.

Webb, F.H. and J.F.Zumberge, And Introduction to GIPSY/OASIS-II, JPL/CALTECH, JPL D-11088, 1997.

Wessel, P. and Smith, W.H.F, New version of the Generic Mapping Tools released, EOS transactions AGU 76, 326, 1995.

Wilson, B.D. ,A. J. Mannucci,and C. D. Edwards, Subdaily Northern-Hemisphere Maps Using An Extensive Network Of GPS Receivers, Radio Science, 30,3, pp. 639-648, 1995.

Zumberge, J.F., D. Dong, M.R. Marcin and D.A. Stowers, Towards a real-time 1-Hz global GPS network, The International Symposium on GPS GPS99 in Tsukuba, Japan, October 1999.